Performance evaluation of multi-stage and multi-pass reverse osmosis networks for the removal of N-nitrosodimethylamine -D6 (NDMA) from wastewater using model-based techniques

M. A. Al-Obaidi [1, 2], C. Kara-Zaïtri [1] and I. M. Mujtaba [1, *]

[1] Chemical Engineering Division, School of Engineering, University of Bradford. Bradford, West Yorkshire BD7 1DP, UK
[2] Middle Technical University, Iraq – Baghdad
***Corresponding author, Tel.: +44 0 1274 233645**
E-mail address: I.M.Mujtaba@bradford.ac.uk

Abstract

The removal of pollutants such as N-nitrosamine present in drinking and reuse water resources is of significant interest for health and safety professionals. Reverse osmosis (RO) is one of the most promising and efficient methodologies for removing such harmful organic compounds from wastewater. Having said this, the literature confirms that the multi-stage RO process with retentate reprocessing design has not yet achieved an effective removal of N-nitrosodimethylamine-D6 (NDMA) from wastewater. This research focuses on this particular challenge and aims to explore several conceptual designs of multi-stage RO processes for NDMA rejection considering model-based techniques and compute the total recovery rate and energy consumption for different configurations of retentate reprocessing techniques. In this research, the permeate reprocessing design methodology is used to increase the process efficiency. An extensive simulation analysis is carried out using high NDMA concentration to evaluate the performance of each configuration under similar operational conditions, thus providing a deep insight on the performance of the multi-stage RO permeate reprocessing predictive design. Furthermore, an optimisation analysis is carried out on the final design to optimise the process with a high NDMA rejection performance and the practical recovery rate by manipulating the operating conditions of the plant within specified constraints limits. The results show a superior removal of NDMA from wastewater.

Keywords: Multi-stage Reverse Osmosis; Permeate Reprocessing; Simulation; Optimisation; N-nitrosamine Rejection; Energy Consumption.

1. Introduction

Water pollution is heightened as a result to industrialization and random discharge of toxic organic compounds from several industrial facilities (Gaikwad and Balomajumder, 2017). N-nitrosodimethylamine-D6 (NDMA) ($C_2H_6N_2O$) is one of many trace organic chemicals present in reclaimed wastewater. NDMA forms as a result to ozonation or chloramination of amine precursors, which are principally associated with wastewater (Krasner *et al.*, 2013, Gwenzi *et al.*, 2018). The formation of N-nitrosamine is quite complex due to several reasons including; the possibility that many reactions occur simultaneously depending on the reactant concentration and the existence of inhibitors (Charrois *et al.*, 2007). NDMA has the lowest molecular weight in the N-nitrosamine family of 74.05. It is considered as one of the most concerning compounds in this family, as it can pose toxicological threats to wildlife and has been classified as a probable carcinogenic compound to human by the US Environmental Protection Agency (US EPA, 2009). The WHO has reported the guideline value of 100 ng/l of NDMA in the water distribution system (WHO, 2008). Resin and zeolites adsorption, activated carbon adsorption, sand filtration and ozonation have a little effect in removing NDMA (Krauss *et al.*, 2010). In terms of the best treatment technology to crush NDMA, UV oxidation is regarded to be the most efficient method. Specifically, a grouping of microfiltration (MF), Reverse Osmosis (RO) and UV/hydrogen peroxide (advanced oxidation processes, AOP) forms the advanced treatment process for the potable reuse of municipal wastewater to degrade NDMA (Gerrity *et al.*, 2013). However, certain utilities observe the re-formation of NDMA in the product water after the oxidation processes as a result to the reactions between NDMA precursors and residual chloramines (Sgroi *et al.*, 2015; McCurry *et al.*, 2017). Amongst all the treatment processes, RO (cheap method) has been widely used in advanced water and wastewater treatment to remove several pollutants, such as harmful trace organics, viruses, and dissolved organic matter (Zhou and Song, 2005; George *et al.*, 2015; Shi et al. 2018). However, the efficacy of the RO process specifically for N-nitrosamine and more importantly for NDMA removal continues to be a challenge as evidenced by a brief state-of-art review in the next sections.

Steinle-Darling *et al*. (2007) tested the rejection of seven N-nitrosoalkylamines using a flat-sheet of three commercial RO membranes. The results showed that NDMA rejection was restricted to 54 – 70% efficiency. Plumlee *et al*. (2008) tested the performance of the RO process to remove

NDMA and concluded that the rejection varied from 24 to 56%. Krauss *et al*. (2010) confirmed that RO can remove NDMA to about 40 – 70%.

Fujioka *et al.* (2012, 2013) used a laboratory-scale system of low pressure NF/RO membranes to investigate the rejection of eight compounds of N-nitrosamine. The results showed that the rejection of NDMA under the same operating conditions ranged between 8 – 80% depending on the type of membrane. Fujioka *et al*. (2014) studied the rejection of N-nitrosamine using full-scale spiral wound RO membrane filtration systems with three and seven pressure vessels PV connected in series respectively (one membrane of 7.9 m^2 per each PV). The study showed that NDMA rejection varies between 40 to 61% and 49 to 35% respectively.

Schäfer *et al*. (2010) claimed that NDMA does not stuck to the membrane properly and indeed remains in the water due to its low hydrophilicity. They affirmed that the rejection of small neutral solutes is mainly due to the NDMA being excluded because of its molecular size. This is MW 74.08 and is in fact can be quite small (depending on compound chemical structure and MW) of 73 Da, which is approximately close to 100 Da MWCO (molecular weight cut off, (Schäfer *et al.*, 2010) of the RO membrane such as Koch membrane. This can possibly explain the poor rejection of NDMA in the RO systems.

It can therefore be argued that the removal of NDMA using laboratory-scale and full-scale RO wastewater treatment process has not proved so far to be entirely efficient and that there is room for improvement.

Several major adjustments in multi-stage seawater RO plant configurations had been examined in the literature. However, one of the best methods for RO superstructure optimisation has been developed by El-halwagi (1992) based on the state space approach, which considered the membrane module type and feed specification. Interestingly, one of the main designs investigated was the permeate reprocessing (two-pass configuration), which was applicable when very high permeate quality is required. For example, Magara *et al.* (1998), Redondo *et al.* (2003) and Farhat *et al*. (2013) deployed this design for the purpose of alleviating the boron concentration in drinking water through the RO desalination process.

To the best of authors' knowledge, the assessment of two-pass configuration for the removal of NDMA from wastewater using the multi-stage RO process has not yet been achieved yet. As explained above, the research community has not directly addressed the performance of different configurations of multi-stage RO wastewater process for removing NDMA. Instead, it seems that

the research community in this field of work focused on studying the impact of operating conditions on the rejection parameter for laboratory and full-scale RO systems. This paper therefore addresses a critical performance assessment using a variety of multi-stage RO designs working in similar operating conditions.

The main aim of this research is to evaluate the performance of different configurations of multi-stage RO wastewater process, including the retentate and permeate reprocessing designs for the improved NDMA removal, the total recovery rate and with the lowest energy consumption using model-based techniques. The secondary aim of this research is to assess the merits of the proposed RO network, which has been specifically designed to include the permeate processing for high NDMA rejection and yet achieve an acceptable permeate recovery rate. However, to the best of the authors' knowledge, no previous study, which utilises the permeate reprocessing design for the multi-stage RO process for the removal of NDMA from wastewater, could be found. The proposed configuration will be further optimised using the optimisation tool of the gPROMS software to determine the highest possible NDMA removal that can be achieved under the practical recovery rate of 40% and lowest energy consumption.

Methodologies

Several mathematical models were developed by Al-Obaidi *et al.* (2016, 2017a, 2017b, 2017c, 2017d, 2017e) and used to quantify the transport phenomenon of water and organic compounds through a single spiral wound RO process. For this paper, a set of algebraic and non-linear equations model were developed based on the above models and used for the removal of NDMA from wastewater. The details of the model used can be found in Table A.1 of Appendix A. Basically, the model assumes the validity of the solution diffusion model with neglecting the impact of fouling in such process due to very low feed concentration of NDMA in wastewater. The model developed is then validated against the actual experimentation of Fujioka *et al.* (2014) of three elements of spiral wound RO process in a series configuration. The model parameters were investigated using the gPROMS software and based on the same experimental data of NDMA removal from wastewater. This include the removal of NDMA from wastewater at two operating pressure of 4, and 6.51 atm. This is also carried out at 2.43E-3 m^3/s, 250 ng/l (2.5E-7 kg/m^3), and 20 ^oC of feed flow rate, NDMA concentration and temperature respectively. Tables A.2 and A.3 in Appendix A show the model parameters and the model validation respectively.

The model showed a negligible error when its prediction values were compared to experimental data. However, the estimated characteristics of the spacer mesh (A' and n) were found to be close to the spacer type CONWED-1 as reported in the study of Da Costa *et al.* (1994) ($A' = 1.29$ and $n = 0.24$).

4. Multi-stage (retentate reprocessing) RO networks description

Seawater desalination plants using RO technology are usually designed as a multi-stage process including three layouts of series, parallel and tapered design. These are usually used to control the plant, quality, and capacity (Schwinge *et al.*, 2004).

The proposed RO industrial full-scale wastewater plant (under investigation) consists of six pressure vessels connected in different configurations of stages. Each stage holds a maximum of six pressure vessels connected in parallel, while each pressure vessel holds a maximum of three spiral wound RO membrane elements type BW30-400 of 37.2 m² produced by Dow/FilmTec and connected in series. The rationale for using three elements per pressure vessel in the proposed design, is to ensure an acceptable range of permeate recovery. This is decreased remarkably depending on the membrane location inside the pressure vessel of similar membranes connected in series. The highest flux always occurs in the first membrane due to the minimum underlying osmotic pressure. The technical specification of the high membrane area used is shown in Table 1. The rationale for selecting this type of membrane is its high NaCl rejection and availability of the technical characteristics, water permeability constant and restricted limits of operation in the literature.

For each proposed layout, a centrifugal high-pressure pump of 80% efficiency that can deliver the wastewater feed at a maximum of 40.463 atm is used. Fig. 1 shows the various configurations of the retentate reprocessing RO network (scenario A – C) test, which will be analysed and assessed for the rejection of NDMA, total permeate recovery and energy consumption. Fig. A.1 in Appendix A shows the rest of the configurations of retentate reprocessing RO network design scenario (D – H), which have been analysed. These configurations are similar in that they use the same retentate reprocessing approach, where the concentrate stream of the first element becomes the feed to the second element and the combined retentate stream of the first stage will be the feed of the second stage. The permeate collected from all the series elements of the pressure vessel are blended with the permeate of other

pressure vessels and then collected with the permeate of the second stage. The statement of working in similar operating conditions is quite applicable for any stage of pressure vessels connected in parallel. It should be noted that most of the configurations presented are similar to those found in an actual industrial plant of the RO seawater desalination process. These configurations used for seawater desalination are based on the design of slightly more elements in the first stage than the following stage. However, the authors have considered the conception of upper and lower limits of operating feed flow rate for each proposed design of multi-stage RO process (6 pressure vessels).

Finally, a simulation model was developed for a spiral wound RO membrane module both in a steady state and multi-stage plant with varying operating parameters along the stages has been implemented using the gPROMS software (General Process Modelling System) developed by the Process System Enterprise Ltd. (2001). The gPROMS Model can be used as a modelling platform for the steady state and dynamic simulation, optimisation, experiment design and parameter estimation. The model equations have been tested and solved for different operating parameters of inlet feed flow rates, pressures, NDMA concentrations and temperatures. In other words, the model is successfully simulated the process within a range of upper and lower limits of the membrane used type (BW30-400) presented in Abbas (2005). The examined simulation ranges are 5 – 40 atm, 0.001 – 0.0053 m³/s, 10 – 45 °C, and trace NDMA concentration to more than 1000 ng/l (1E-6 kg/m³) of operating pressure, feed flow rate, temperature, and concentration respectively. Moreover, the model is able to estimate the performance of an individual spiral wound RO process for the removal of any different compound at different operating conditions in case of manipulating the mass transport characteristics and mass transfer coefficient correlation.

Table 1. Specifications of the spiral wound membrane element (Abbas, 2005)

Make	Dow/FilmTec
Membrane type and configuration	BW30-400, Spiral-wound, Polyamide Thin-Film Composite
Feed and permeate spacer thickness t_f (m)	5.93E-4
Hydraulic diameter of the feed spacer channel d_h (m)	8.126E-4
Effective membrane area A (m²)	37.2
Membrane length L and width W (m)	1 and 37.2
$A_{w\,(T_o)}$(m/ atm s) at 28.8 °C	9.5096E-07
$B_{s(T_o)}$ (NDMA) (m/s) at 20 °C	5.35E-6*
Mwt_{NDMA} (kg/kmol) *	74.05
Spacer type	(NALTEX-151-129)
$A^{'}$ (dimensionless)	7.38

n (dimensionless)	0.34
ε (dimensionless)	0.9058

*: Fujioka *et al.* (2014).

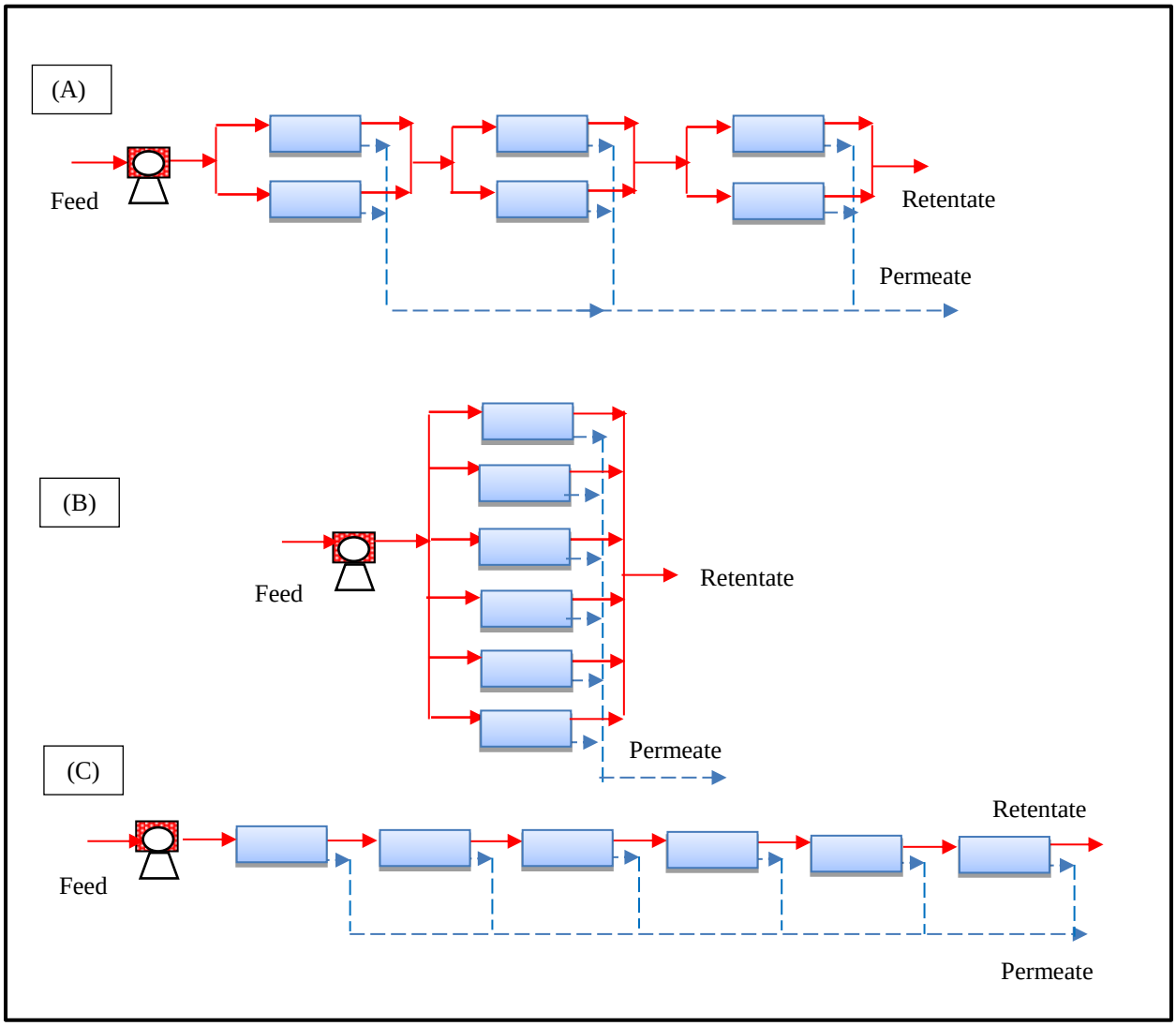

Fig. 1. The tested configurations of retentate reprocessing RO networks of six pressure vessels

4.1 Problem specifications: Steady state simulation

In this section, the effect of six pressure vessel configurations shown in Fig. 1 on the NDMA rejection Rej_{plant}, total permeate recovery Rec_{plant} and total energy consumption $E1$ is analysed by simulation study. This is carried out using the selected operating conditions of 1E-6 kg/m³ (1000 ng/l), 13 atm, 8.9E-3 m³/s, 25.3 °C of inlet feed concentration, pressure, flow rate and temperature respectively. Despite the Ministry of the Environment (MOE) of Ontario has

regulated the allowable concentration of NDMA in drinking water at 9 ng/l (Ministry of the Environment of Ontario, 2009), the occurrence of NDMA in the treated water ranges between 30 to 700 mg/l as a result to ozonation process (Andrzejewski *et al.*, 2008). Najm and Trussell 2001 confirm that the NDMA formation can exceed 100 ng/l during chlorination of secondary wastewater effluent. However, wastewater and sewage water often contain significant concentrations of NDMA. The NDMA concentration of the samples collected from 20 sewage treatment plant is between non-detectable to 1000 ng/l (Krauss *et al.*, 2009). Fujioka *et al.* (2014) used approximately 250 ng/l as a feed concentration of NDMA in the experimental work of a pilot-scale RO plant of three stages connected in series. More recently, Fujioka *et al.* (2018) have used 1000 ng/l as NDMA concentration in the experiments of removal NDMA by modified three commercial RO membranes. Therefore. The authors selected 1000 ng/l of NDMA concentration as it represents the maximum concentration that can be found in wastewater. Also, the RO process considering wastewater is usually working at the range of medium pressures between 10 to 20 atm and depending on the upper limit of the membrane module, which is already considered in this simulation. Fujioka *et al.* (2014), Sundaramoorthy *et al.* (2011) and Srinivasan *et al.* (2009, 1010, 2011) use the range of 5 to 15 atm for the removal of NDMA, chlorophenol, dimethylphenol and phenol from wastewater. It is noteworthy to mention that the analysis of the performance of these layouts using high membrane area of 37.2 m² has not been investigated in the literature. Table 2 and Table A.4 in Appendix A summarise the simulation results of the selected configurations of multi-stage RO process shown in Fig. 1 and Fig. A.1 in Appendix A. Table 2 and Table A.4 in Appendix A show the poor rejection of the selected configurations (A – H).

Table 2. Simulation results of seventeen scenarios of retentate reprocessing RO networks

Scenario	Rej_{plant} (-)	Rec_{plant} (-)	$E1$ (kWh/m³)
A	40.429	72.900	0.627
B	38.691	79.155	0.578
C	40.527	34.368	1.331

5. Multi-pass (permeate reprocessing) RO networks description

To overcome the problem of poor NDMA rejection presented in Table 2 and Table A.4 in Appendix A of the analysed configurations shown in Fig. 1 and Fig. A.1 in Appendix A, the objective of this section is to use a permeate reprocessing technique that assumes the blending of

the collected permeate of stage 1 and feed it to stage 2 and so on. The high-pressure retentate streams are blended from each stage and pass through ERD to pressurise the low-pressure permeate streams and then reject them out. This approach is pragmatic but reasonable since the flow rate of the blended permeate stream of stage 1 will be within the allowable limits of the feed flow rate of the membranes in stage 2. Fig. 2 shows a schematic diagram of three stages of the permeate reprocessing technique under investigation. The RO layout presented in Fig. 2 includes the energy recovery device ERD, which is required to transfer the pressure energy of high concentrated streams into the low-pressure permeate streams. The current model did not include any pumps, which are associated with high installation, operation, and maintenance costs. However, despite increasing the capital cost of treatment, it is expected that the power consumption of the multi-pass RO system will be reduced because of the energy recovery device ERD. To study the performance of permeate reprocessing design and to compare with other selected configurations of Fig. 1 and Fig. A.1 in Appendix A, the model of the new layout of permeate reprocessing technique has been simulated using the same operating conditions shown in Section 4.1. The final simulation results of scenario I are shown in Table 3.

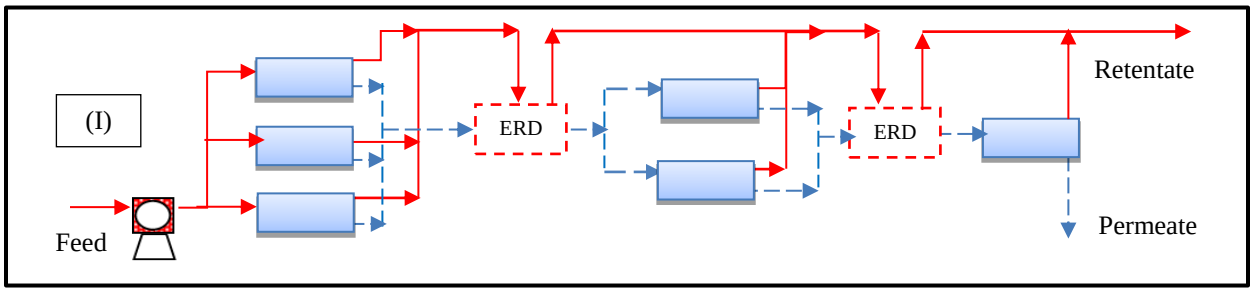

Fig. 2. Tested configuration of permeate reprocessing RO network of three stages

A close look at the results shows that a poor recovery rate of the proposed permeate reprocessing technique of scenario I (Table 3), and this can be considered as the main drawback of this design. The reason for this is the disposing of the retentate streams of higher flow rate of the treatment system. Having said this, it is noteworthy to mention that configuration G shown in (Fig. A.1 – Appendix A) has given one of the highest permeate recovery (Table A.4 – Appendix A), which has been selected for further validity and performance analysis of the permeate reprocessing design. The schematic diagram of permeate reprocessing of two stages of 4 and 2 parallel

pressure vessels respectively can be found in Fig. 3 (scenario J). Also, configurations K and L (Fig. 4) use both retentate and permeate reprocessing design. The three proposed configurations J, K and L are simulated using the same operating conditions mentioned in Section 4.1. The final simulation results are shown in Table 3.

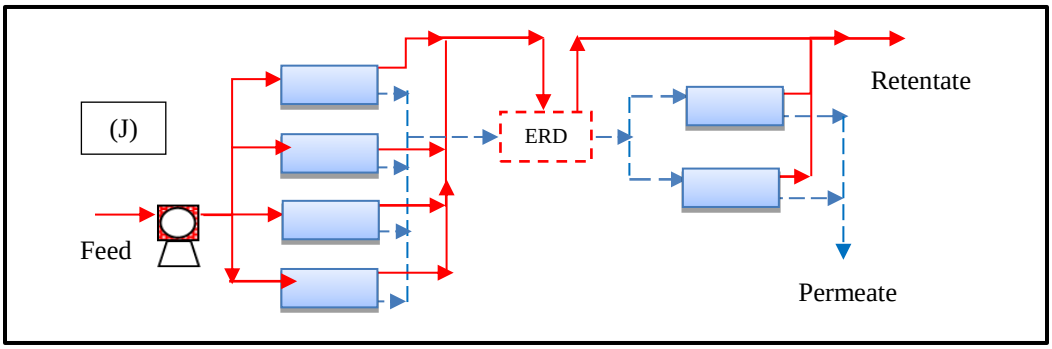

Fig. 3. Tested configuration of permeate reprocessing RO network of two stages

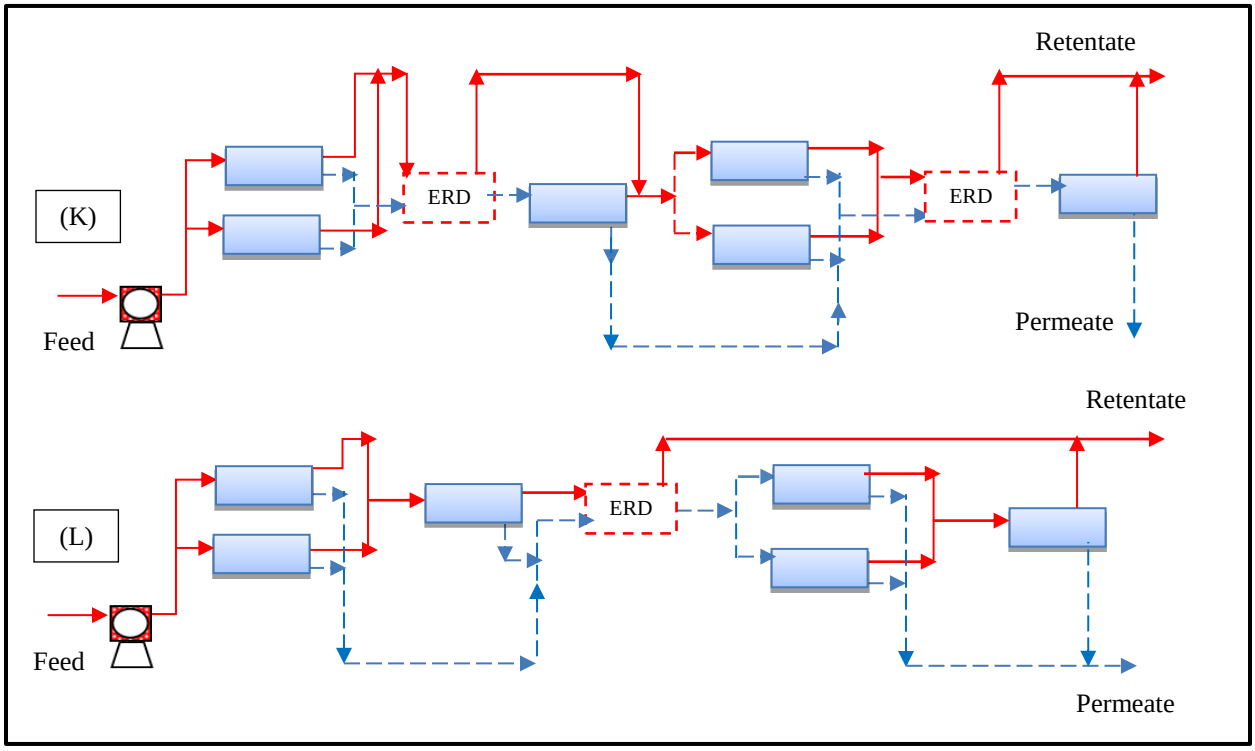

Fig. 4. Tested two configurations of retentate and permeate reprocessing RO network of four stages

Table 3. Simulation results of permeate reprocessing RO networks

Scenario	Rej_{plant} (-)	Rec_{plant} (-)	$E2$ (kWh/m³)
I	85.035	9.941	3.276
J	73.120	22.920	1.323
K	76.078	8.617	1.173
L	68.060	27.283	0.766

6. Discussion of multi-stage RO process design performance

The evaluation of the performance of multi-stage RO process design is addressed in this section. Despite using the same operating conditions for testing the retentate reprocessing scenarios A to C shown in Fig. 1 and D to H in Fig. A.1 in Appendix A, it is notable that the configurations tested have achieved NDMA rejection ranging between 38.69 and 40.52% (Table 2 and Table A.4 in Appendix A). The total recovery rate and energy consumption range between 34.3 and 79.15%, and 0.578 and 1.33 kWh/m³ respectively. However, configuration A is the optimal arrangement that show the best performance of NDMA rejection (Table 2). Configuration A has only two pressure vessels at the first stage, seemingly linked to higher performance of NDMA rejection. Nevertheless, the highest plant recovery and lowest energy consumption result from using configurations G, H (Fig. A.1 – Appendix A) and B (Fig. 1). These configurations are designed with the high number of parallel pressure vessels at stage 1 compared to other configurations tested. This can be explained by the higher feed pressure implemented for each compartment, which lifts the water flux through the membrane and increases the total permeate recovery. It is noteworthy to mention that the recovery rate of these layouts positively increases as the number of pressure vessels of the first stage increases (Table 2). G, H (Fig. A.1 – Appendix A) and B (Fig. 1) configurations are based on a parallel connection of 4, 5 and 6 pressure vessels respectively at the first stage. However, their performance of NDMA rejection yields one of the lowest scores. The main characteristic of this configuration is that the feed flow rate is immediately reduced for each compartment due to splitting it into a number of streams, which lowers the bulk velocity and the Reynold number. This is in turn reduces the mass transfer coefficient, which ultimately increases the accumulation of solute over the membrane and results in higher solute flux, which reduces the rejection parameter. Additionally, the series

configuration C (Fig. 1) has the lowest total recovery and the highest energy consumption in comparison to other investigated layouts. This might be explained by the high feed flow rate, which is accompanied by a higher pressure drop and a lower permeate recovery, which in turn increase the total energy consumption. Fujioka *et al*. (2014) has tested the series superstructure of seven elements of membrane area of 7.9 m² and proved an abatement of NDMA removal. Table 2 shows that the design of one pressure vessel in the first stage yields a higher NDMA rejection, which is similar to those obtained for configuration C (Fig 1). This is because this configuration has the highest feed flow rate in the first stage, which corresponds to a higher turbulence in the feed channel and a lower concentration polarisation, which in turn increases NDMA rejection. The same findings are confirmed by Farhat *et al*. (2013) for the case of boron rejection.

Among the evaluated configurations of Fig. 1, the permeate reprocessing design shown in Figs. 2 and 3 and the coupling permeate and retentate reprocessing design shown in Fig. 4 have undoubtedly a higher competitive design performance. However, the issue of lower permeate recovery of configuration I can be relatively solved by implementing the design of configuration J of permeate reprocessing design with four pressure vessels in stage 1, which in turn passively impacts on the rejection parameter and positively reduces the energy consumption. Also, the results of the coupling of retentate and permeate reprocessing designs of Fig. 4 (configurations K and L) confirm its differentiated quality for the NDMA rejection indicators tested, in respect of, the total permeate recovery and energy consumption. Specifically, configuration K offers a higher rejection than configuration L. However, configuration L comes with higher recovery rate and lower energy consumption compared to configuration K.

It is concluded therefore, that the permeate reprocessing design yields a lower permeate recovery. This implies further work to investigate a new design to resolve this issue by adjusting the removal of NDMA and lifting the total permeate recovery to the acceptable value of 40%.

7. Predictive permeate reprocessing multi-pass RO process design

The successive successful performance of the permeate reprocessing approach shown in Table 3 has provided a stimulus to select this technique for achieving higher NDMA rejection together with a feasible total permeate recovery. Thus, the objective of this section is to show the use of a simple predictive design of permeate reprocessing of multi-pass RO design (scenario M) shown

in Fig. 5, which can achieve this. A trial-and-error design method has been adopted to identify the best network and stream connections considering the permeate reprocessing. In the current work, a multi-stage superstructure of twelve pressure vessels, two pumps and three energy recovery devices were adopted as can be shown in Fig. 5. The restriction of lower and upper limits of operating parameters of feed flow rate and feed pressure for each membrane element has been mainly considered along the design of this network. Therefore, stages S1, S2, S5 and S6 have three membrane elements connected in series for each pressure vessel, while stages S3 and S4 contain only one element for each pressure vessel. The idea behind the second pump is to feed the collected permeate of stage 2 to stage 5 with high feed pressure for ultra-filtration purposes. While, the retentate stream of stage 2 is fed directly to stage 3 to overcome the problem of low recovery rate. Moreover, the use of an energy recovery device is to ensure the transferring of potential energy from the high-pressure side to the low-pressure side considering the efficiency of the ERD.

The simulation of the proposed network design shown in Fig. 5 is conducted using the same operating condition given in Section 4.1. The simulation results show a remarkable increase in the rejection of NDMA recorded at 87.13% by acquiring 11.172 % and 3.19 as total permeate recovery and energy consumption respectively. It is worthy to mention that the two pumps of configuration M are working on a similar operating pressure of 13 atm along this simulation.

It is clearly recognised that the recovery rate of the new proposed configuration of permeate reprocessing is still in issue of this design, which is occurring as a result of several permeate reprocessing steps. However, the result of NDMA rejection is comparable with the findings of the previous configurations tested. Also, the effectiveness of the permeate reprocessing technique has confirmed the significance of employing this method to meet high NDMA rejection. Moreover, there is a capacity now for optimising the process to acquire the preferable permeate recovery of 40% under lower total energy consumption. This is dealt with in the next section.

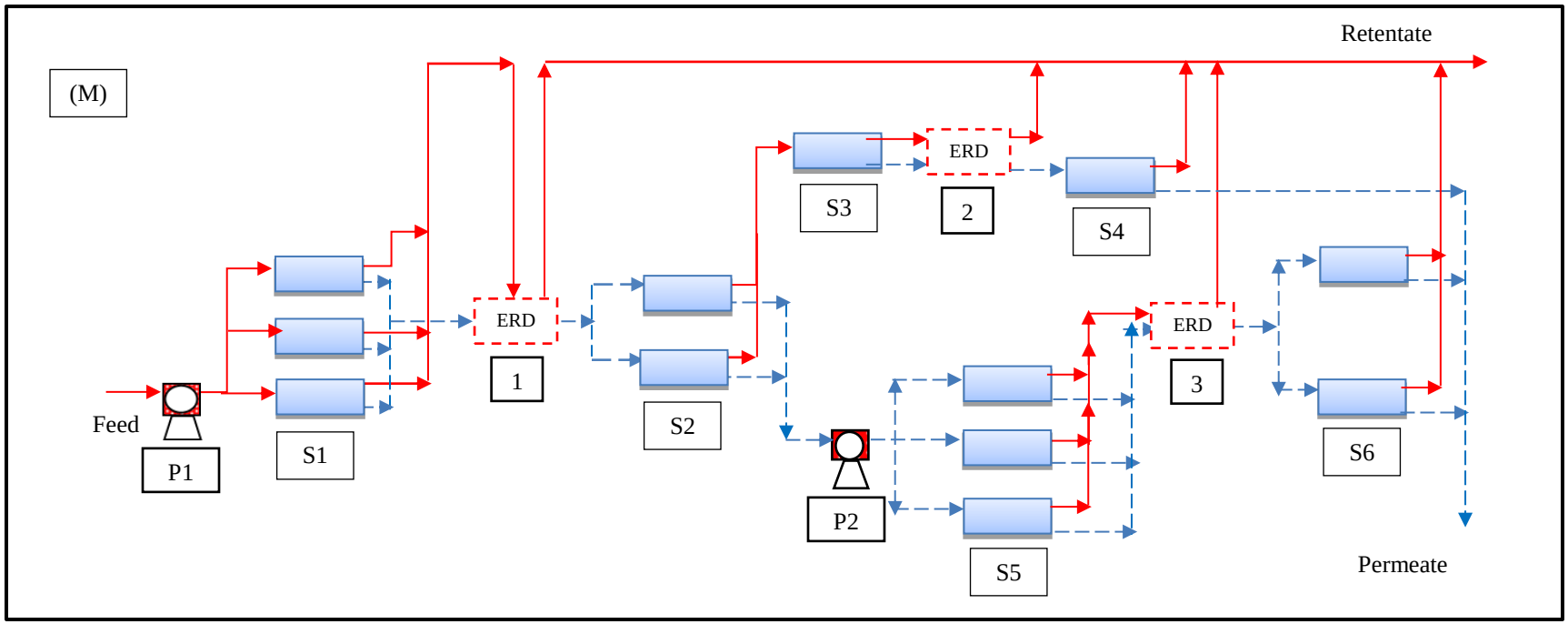

Fig. 5. Six stages RO network with permeate reprocessing, P: Pump, S: Stage, ERD: Energy recovery device

8. Optimisation of predictive multi-pass permeate reprocessing RO process design

The optimisation of the permeate reprocessing design of multi-pass RO process shown in Fig. 5 is carried out using the gPROMS software. Mathematically, this optimisation is corresponding to solving a purely algebraic problem in which a general nonlinear objective function is maximised or minimised subject to general nonlinear constraints by deploying a set of optimisation decision variables that may be either continuous or discrete. Therefore, the process model (nonlinear algebraic equations) presented in Section 2 can be written in the following compact form:

$f(x, u, v) = 0$

Where, x is the set of all algebraic variables, u is the set of decision variables (to be optimised) and v denotes the constant parameters of the process. The function f is assumed to be continuously differentiable with respect to all their arguments.

The gPROMS software offers an optimisation tool, which can predict the appropriate operating conditions precisely, and these will confirm the outstanding performance of the network.

8.1 Problem description and formulation

The objective of this section is to find optimum operating conditions of the plant shown in Fig. 5 using the optimisation tool of the gPROMS software for NDMA rejection, total permeate recovery and total energy consumption. Therefore, the optimisation problem is to maximise the NDMA rejection under the feasible recovery rate of 40% for the predictive design of permeate reprocessing of Fig. 5, by allowing the system operating conditions of the plant ($Q_{f(plant)}$, $P_{f(in)(plant)}$, $P_{f(in)(S5)}$ and $T_{(plant)}$) to vary within the constraints of upper and lower limits. Specifically, the inlet feed flow rate of the plant $Q_{f(plant)}$ was established within the minimum and the maximum sum of three elements connected in a parallel configuration. Moreover, the optimisation problem has considered the manufacturer's specifications of each single spiral-wound RO membrane element in the proposed network and reported in Table 4, which offer the maximum and minimum practical bounds of operating conditions including; inlet feed pressure $P_{f(in)}$ and feed flow rate Q_f. These constraints provide a safe operation of the RO process. A range of 20 to 30 °C was considered as the upper and lower limits of inlet feed temperature $T_{(plant)}$ without considering the higher limit of 45 °C (case 1). This choice is quite acceptable for a steady-state operation of the RO system and elucidated a long-life of the membranes. Also, a constraint of 0.987 atm has been set as a maximum allowable pressure drop

ΔP_{drop} (atm) along each membrane element commensurate with the supplier's specifications. The optimisation is investigated for inlet high feed concentration of 1000 ng/l, which is equivalent to 1E-6 kg/m³ of NDMA. Also, the optimisation problem is formulated as a Non-Linear Problem (NLP) with process and module constraints. To examine the viability of the proposed configuration, a maximum value of 40% of total permeate recovery $Rec_{(plant)}$ has been chosen as a stringent limit of optimisation problem to avoid increased energy consumption considering the technical specification and capacity of seawater reverse osmosis desalination plant (Peñate *et al.*, 2011). In other words, several researchers show the feasibility of 40% of total water recovery as an effective operational strategy for the RO seawater desalination plants (Loutatidou *et al.*, 2017). Therefore, this value has been taken to consider high quality of total recovery for such small size of wastewater RO plant, which implemented multi-pass RO design. This type of design promotes the removal of pollutants on the penalty of losing the permeate recovery. Also, it should be noted that the used membrane (BW30-400), which is already used in brackish water desalination, can resist a total of operating pressure of 40.4 atm (Abbas, 2005). This is compared to what can be seen in seawater desalination RO process where the operating pressure exceeds 79 atm (Ghobeity and Mitsos, 2010). The total energy consumption $E2$ was constrained with a maximum of 3 kWh/m³ to ensure lower energy consumption. Occasionally, large scale seawater RO plants have an energy consumption of roughly 3.5 kWh/m³ (Wei *et al.*, 2017).

Therefore, the optimisation problem of the RO process with permeate reprocessing is addressed in this work as described below:

Given: Operating feed conditions, module specifications.

Optimise: Inlet feed pressure, flow rate, temperature, and inlet feed pressure of stage 5 (the optimisation variables).

Maximize: NDMA rejection.

Subject to: Equality (process model) and inequality constraints (linear bounds of optimisation variables).

Precisely, the optimisation problem is mathematically represented as follows:

$$\underset{Q_{f(plant)},\, P_{f(in)(plant)},\, P_{f(in)(S5)},\, T_{(plant)}}{Max} \quad Rej_{(NDMA)}$$

Subject to:

Equality constraints:

Process Model $f(x, u, v) = 0$

Inequality constraints of the plant:

$$Q_{f(plant)}{}^{L} \leq Q_{f(plant)} \leq Q_{f(plant)}{}^{U}$$

$$P_{f(in)(plant)}{}^{L} \leq P_{f(in)(plant)} \leq P_{f(in)(plant)}{}^{U}$$

$$P_{f(in)(S5)}{}^{L} \leq P_{f(in)(S5)} \leq P_{f(in)(S5)}{}^{U}$$

$$T_{(plant)}{}^{L} \leq T_{(plant)} \leq T_{(plant)}{}^{U}$$

Inequality constraints of the element:

$$Q_f{}^{L} \leq Q_f \leq Q_f{}^{U}$$

$$P_{f(in)}{}^{L} \leq P_{f(in)} \leq P_{f(in)}{}^{U}$$

$$T^{L} \leq T \leq T^{U}$$

$$\Delta P_{drop} \leq 0.987$$

$$Rec_{(plant)} \geq 40\%$$

$$E2 < 3.0$$

The optimisation results of case 1 shows an energy consumption of 2.664 kWh/m³ (Table 5). Therefore, the sensitivity of optimisation technique will be subjected to the highest supplier's limit of feed temperature of 45 °C and a new constraint of energy consumption of lower than 2.664 kWh/m³ to investigate its impact on the plant performance (case 2). Therefore, the optimisation limits of operating temperature are amended, and the energy consumption constraint is added as follows:

$$E2 < 2.664$$

Table 4. The limits of operation of the spiral-wound membrane element (Abbas, 2005)

Parameter	Value
Max. operating temperature T (°C) of case 1	30
Max. operating temperature T (°C) of case 2	45
Max. operating pressure $P_{f(in)(plant)}$ (atm)	40.463
Max. pressure drop ΔP_{drop} (atm)	0.987
Max. feed flow rate Q_f (m³/s)	5.363E-3
Min. feed flow rate Q_f (m³/s)	1.008E-3

8.2 Optimisation results of predictive multi-pass permeate reprocessing RO design

The optimisation results of configuration M shown in Fig. 5 regarding the optimisation cases 1 and 2 are shown in Table 5. It is noticeable that the proposed configuration can offer higher NDMA rejection $Rej_{(NDMA)}$ of 92.487% in case 1 together with by 40% and 2.664 kWh/m³ of total permeate recovery rate $Rec_{(plant)}$ and energy consumption $E2$ respectively, compared to all configurations tested and shown in Figs. 1, 2, 3 and 4. Interestingly, this offers a permeate concentration of only 75 ng/l (Table 5), which is within the restricted limits of 100 ng/l of WHO (WHO, 2008). However, the impact of feed temperature can be shown in case 2 (A and B), which illustrated two competing options of optimum operating conditions and shows fairly similar NDMA rejection at lower energy consumption than in case 1. This behaviour can be ascribed to the fact that the operating plant temperature has a considerable impact on both permeate $A_{w(T)}$ and NDMA $B_{s(T)}$ permeability constants of the membrane as illustrated in Eqs. (28) and (29) respectively. Increasing the feed temperature to 36 and 41.633 °C will increase the water permeability constant and decrease the viscosity of water, which in turn increase the amount of water that pass through the membrane, which ultimately results in reducing the energy consumption. However, increasing the feed temperature to 36 °C causes an increase in the NDMA flux through the membrane caused by the thermodynamic increase in the NDMA osmotic pressure as a result to an increase in the NDMA permeability constant, which reduces the rejection parameter to 92.375% (permeate concentration=76 ng/l). The same findings are confirmed by Farhat *et al*. (2013) where the boron rejection decreases as the feed temperature increased. Also, it seems that expanding the optimisation limit of the operating temperature to 45 °C and introducing a new constraint of energy consumption of less than 2.664 kWh/m³ causes a selection of a higher feed temperature of 36 °C in case 2A, which requires an adjustment for both the operating pressures of the plant and stage 5 as well as the inlet feed flow rate to keep a constraint of 40% total recovery rate as a constraint. As a result, an increase of the feed pressure of stage 5 is mandatory to guarantee a sufficient driving force for permeate flux to maintain 40% total recovery, especially after increasing the operating feed flow rate, which causes a higher pressure drop due to a higher friction along the membrane length. Specifically, an increase in the

inlet feed flow rate causes a decrease in the water flux and total permeate recovery, which negatively impacts the removal of NDMA to 92.375%.

In contrast, increasing the operating feed temperature to 41.633 °C in case 2B causes an increase in the mass transfer coefficient, which increases the rejection parameter to 93.11% (permeate concentration=69 ng/l) by reducing the concentration polarisation impact. However, the optimisation process has resulted in an increase of the inlet feed flow rate in a way to maintain the total recovery of 40% and keep the consumption of energy lower than 2.664 kWh/m^3, and this has a positive impact on the rejection parameter. It can be argued therefore that the adapted design is a more effective technique for NDMA removal, which meets both the satisfactory recovery rate and energy consumption.

More importantly, the optimised results shown in Table 5 is so promising especially after the experimental research that has been done by Fujioka *et al.* (2018). This research has improved the NDMA removal from wastewater to 92% after using a complex heat treatment method on the prototype RO membrane. However, this result is commensurate with a reduction of water permeability constant in the range between 21 to 31%, which shows very low recovery rate.

Finally, there is no doubt that there are several treatment methods including; adsorption, activated carbon, metal complexation, hydrolysis, ozonation and ultraviolet photolysis (Lee *et al.*, 2005), used for the removal of pollutants from wastewater. However, the efficient standard treatment procedures used for N-nitrosamine removal from recycled water including; coagulation with ferric chloride, disinfection by chloramination, ultrafiltration (UF), reverse osmosis (RO), and an ultraviolet radiation-hydrogen peroxide advanced oxidation process (UV/H_2O_2) is successfully implemented in several indirect potable water reuse schemes (Steinle-Darling *et al.*, 2007). However, the main concern of this process is the high treatment cost caused by the necessity of using high dose of UV radiation to remove NDMA removal compared to lower dose used for other organic pollutants. Therefore, it is important to investigate in future the capital and operating cost of the proposed RO design for comparison purposes. In this respect, the disposal of retentate high NDMA concentration stream of RO membrane is a growing concern. To systematically resolve this, it would be interesting to experimentally investigate the feasibility of the combination of UV irradiation in the presence of titanium dioxide treatment (UV/TiO_2) and simple sand filter biological system proposed by Westerhoff et al. (2009). This method can

effectively degrade the organic compounds concentration such as NDMA and which ultimately means of reducing its potential environmental impact.

Table 5. Optimisation results of configuration V at feed concentration of 1000 ng/l of NDMA

Case		The decision variables				$Rej_{(NDMA)}$ (-)	$Cp_{(NDMA)}$ (ng/l)	$Rec_{(plant)}$ (-)	$E2$ (kWh/m³)
		$Q_{f(plant)}$ (m³/s)	$P_{f(in)(plant)}$ (atm)	$P_{f(in)(S5)}$ (atm)	$T_{(plant)}$ (°C)				
1		7.9526E-3	23.504	40.463	30.000	92.487	75.13	40.000	2.664
2	A	8.4510E-3	22.201	38.109	36.000	92.375	76.25	40.000	2.500
	B	9.8887E-3	23.390	40.033	41.633	93.110	68.9	40.001	2.612

9. Conclusions

Different configurations multi-stage wastewater retentate reprocessing RO systems have been proposed and evaluated in terms of plant performances including; NDMA removal, total permeate recovery and energy consumption considering model-based approach. In order to further improve the performance of the initial configurations presented, a smart permeate reprocessing technique has been developed for removing NDMA from wastewater and validated. An associated simulation study has also been implemented and achieved similar operating conditions. it has enabled the assessment of the performance of both retentate and permeate reprocessing designs and confirmed the significance of lower NDMA rejection of retentate design. The research results clearly show that the proposed adaptive RO design with permeate reprocessing was able to solve this issue and will not doubt lead the way for further studies to achieve the full removal (zero discharge) of NDMA. The technique developed includes a novel design for the removal of NDMA from wastewater in a multi-stage reverse osmosis process. This design has been compared with a variety of configurations and confirmed its validity of higher performance based on three tested indicators. The results readily confirm that the proposed design is suitable for removing this carcinogenic compound for water reuse. Specifically, it has been found that the RO permeate reprocessing design process can significantly enhance the removal of NDMA from wastewater. Also, the optimisation of the proposed design yields a competitive value of 92.49% rejection and a practicable permeate recovery of 40% at an all-time low 2.664 total energy consumption. Interestingly, with the inlet feed concentration of 1000 ng/l,

the proposed RO configuration can reduce the permeate concentration to lower than the restricted limits of 100 ng/l of WHO. This is compared to the maximum NDMA rejection of 92% at a considerable reduction of water transport parameter of 21 to 31% for several tested membrane types as a result to the use of heat treatment method on the membrane tested (Fujioka *et al.*, 2018). The simulation and optimisation framework has been carried out using a set of nonlinear algebraic equations to model the membrane transport phenomena and NDMA rejection. The prediction of the model developed was compared to a pilot-scale experimental data from the literature and shows an excellent corroboration with small discrepancies.

It must be noted that the proposed RO configuration has not been used in practice yet to remove NDMA from wastewater and remain therefore theoretical at this stage.

Nomenclature

A : Effective area of the membrane (m²)

$A_{w(T)}$: Solvent transport coefficient at any temperature (m/atm s)

A' : The spacer characteristics (dimensionless)

$B_{s(T)}$: Solute transport coefficient at any temperature (m/s)

C_b : The bulk feed solute concentrations at the feed channel (kg/m³)

C_f : The inlet feed solute concentrations at the feed channel (kg/m³)

C_w : The solute concentration on the membrane surface at the feed channel (kg/m³)

C_p : The permeate solute concentration at the permeate channel (kg/m³)

C_r : The retentate concentration of a membrane module (kg/m³)

C_{td} : The total drag coefficient (dimensionless)

D_b : The solute diffusion coefficient of feed at the feed channel (m²/s)

d_h : The hydraulic diameter (m)

$E1$: The total energy consumption of the plant with only high-pressure pump (kW h/m³)

$E2$: The total energy consumption of the plant with high-pressure pump and ERD (kW h/m³)

J_s : The solute molar flux through the membrane (kg/m² s)

J_w : The permeate flux (m/s)

k : The mass transfer coefficient at the feed channel (m/s)

K : The efficiency of mixing net (i.e. spacer) (dimensionless)

L : The length of the membrane (m)

m_f : Parameter in Eq. (10) of Table A.1

Mwt : Molecular weight (g/mol)

n : The spacer characteristics (dimensionless)

$P_{f(in)}$: The inlet feed pressure of a membrane module (atm)

$P_{f(in)(ERD)}$: The inlet pressure of ERD (atm)

$P_{f(in)(plant)}$: The inlet pressure of the plant (atm)

$P_{f(in)(S5)}$: The inlet pressure of stage 5 (atm)

$P_{f(out)}$: The retentate pressure of a membrane module (atm)

$P_{f(out)(ERD)}$: The outlet pressure of ERD (atm)

P_p : The permeate channel pressure of a membrane module (atm)

Q_b : The bulk feed flow rate at the feed channel of a membrane module (m^3/s)

Q_f : The inlet feed flow rate at the feed channel of a membrane module (m^3/s)

Q_p : The permeate flow rate at the permeate channel of a membrane module (m^3/s)

Q_r : The retentate flow rate at the feed channel of a membrane module (m^3/s)

Re : The Reynold number at the feed channel (dimensionless)

Rec : Total permeate recovery of a membrane module (dimensionless)

$Rec_{(plant)}$: The total recovery rate of the plant (dimensionless)

Rej : The solute rejection coefficient of a membrane module (dimensionless)

$Rej_{(NDMA)}$: The plant total rejection of NDMA (dimensionless)

T : The feed temperature of a membrane module (°C)

T_0 : The reference temperature (°C)

$T_{(plant)}$: The inlet feed temperature of the plant (°C)

t_f : Height of feed channel (m)

U_b : The bulk feed velocity at the feed channel of a membrane module (m/s)

W : The membrane width (m)

Subscript

μ_b : The Feed viscosity at the feed channel of a membrane module (kg/m s)

ρ_b : The feed density at the feed channel of a membrane module (kg/m³)

ΔL : The characteristic length of mixing net (m)

ΔP_{drop} : The pressure drop of the spiral wound element (atm)

$\Delta \pi_{Total}$: The osmotic pressure difference (atm)

π_w : The osmotic pressure at the membrane wall (atm)

π_p : The osmotic pressure at the permeate channel (atm)

ε_{pump} : Pump efficiency (dimensionless)

ε_{ERD} : Energy recovery device efficiency (dimensionless)

ϵ : The void fraction of the spacer (dimensionless)

References

Abbas, A. Simulation and analysis of an industrial water desalination plant. *Chemical Engineering and Processing*, 2005, 44, 999–1004.

Al-Obaidi, M. A.; Kara-Zaïtri, C.; Mujtaba I. M. Development and Validation of N-nitrosamine Rejection Mathematical Model Using a Spiral-wound Reverse Osmosis Process. *Chemical Engineering Transactions*, 2016, 52, 1129–1134.

Al-Obaidi, M. A.; Li, J- P.; Kara-Zaïtri C.; Mujtaba I. M. Optimisation of reverse osmosis based wastewater treatment system for the removal of chlorophenol using genetic algorithms. *Chem. Eng. J.* 2017a, 316, 91–100.

Al-Obaidi, M. A.; Kara-Zaïtri, C.; Mujtaba, I. M. Removal of phenol from wastewater using spiral-wound reverse osmosis process: Model development based on experiment and simulation. *Journal of Water Process Engineering*, 2017b, 18, 20–28.

Al-Obaidi, M. A.; Kara-Zaitri, C.; Mujtaba, I. M. Modeling of a spiral-wound reverse osmosis process and parameter estimation. *Desalination and Water Treatment*, 2017c, 69, 93–101.

Al-Obaidi, M. A.; Kara-Zaïtri, C.; Mujtaba, I. M. Optimisation of membrane design parameters of a spiral-wound reverse osmosis module for high rejection of dimethylphenol from wastewater at low energy consumption. In Computer Aided Process Engineering-40, Espuna et al. (editors), 2017, 2713-2718.

Al-Obaidi, M. A.; Kara-Zaïtri, C.; Mujtaba, I. M. Simulation of full-scale reverse osmosis filtration system for the removal of N-nitrosodimethylamine from wastewater. *Asia-Pacific Journal of Chemical Engineering*, 2017e, e2167, 1–13.

Andrzejewski, P.; Kasprzyk-Hordern, B.; Nawrocki, J. N-Nitrosodimethylamine (NDMA) formation during ozonation of dimethylamine containing water. *Water Res.* 2008, 42, 863–870.

Charrois, J. W. A.; Boyd, J. M; Froese, K. L.; Hrudey, S.E. Occurrence of N-nitrosamines in Alberta public drinking-water distribution systems, *Journal of Environmental Engineering and Science*, 2007, 6(1), 103–114.

Da Costa, A. R.; Fane, A. G.; Wiley, D. E. Spacer characterization and pressure drop modelling in spacer-filled channels for ultrafiltration. *J. Membr. Sci.* 1994, 87, 79–98.

El-halwagi, M. M. Synthesis of reverse osmosis networks for waste reduction. *AICHE Journal*, 1992, 38, 1185–1198.

Farhat, A.; Ahmad, F.; Hilal, N.; Arafat, H.A. Boron removal in new generation reverse osmosis (RO) membranes using two-pass RO without pH adjustment. *Desalination*, 2013, 310, 50–59.

Fujioka. T.; Nghiem. L.D.; Khan. S.J.; Mcdonald. J. A.; Poussade. Y.; Drewes. J. E. Effects of feed solution characteristics on the rejection of N-nitrosamines by reverse osmosis membranes. *J. Membr. Sci.* 2012, 409–410**,** 66–74.

Fujioka, T.; Khan, S.J.; Mcdonald, J.A.; Roux, A.; Poussade, Y.; Drewes, J.E.; Nghiem, L.D. N-nitrosamine rejection by nanofiltration and reverse osmosis membranes: The importance of membrane characteristics. *Desalination*, 2013, 316**,** 67–75.

Fujioka, T.; Khan, S.J.; Mcdonald, J.A.; Roux, A.; Poussade, Y.; Drewes, J.E.; Nghiem, L.D. Modelling the rejection of N-nitrosamines by a spiral-wound reverse osmosis system: Mathematical model development and validation. *J. Membr. Sci.* 2014, 454, 212–219.

Fujioka, T. ; Ishida, K. P. ; Shintani, T. ; Kodamatani, H. High rejection reverse osmosis membrane for removal of N-nitrosamines and their precursors. *Water Res.* 2018, 131, 45–51.

Gaikwad, M.S.; Balomajumder, C. Simultaneous rejection of chromium(VI) and fluoride [Cr(VI) and F] by nanofiltration: Membranes characterizations and estimations of membrane transport parameters by CFSK model. *Journal of Environmental Chemical Engineering,* 2017, 5, 45–53.

George, J. S., Ramos, A.; Shipley, H.J. Tanning facility wastewater treatment: Analysis of physical–chemical and reverse osmosis methods. *Journal of Environmental Chemical Engineering*, 3, 2015, 969–976.

Gerrity, D.; Pecson, B.; Trussell, R.S.; Trussell, R.R. Potable reuse treatment trains throughout the world. *J. Water Supply: Res. Technol*.—AQUA, 62, 2013, 321–338.

Ghobeity, A.; Mitsos, A. Optimal time-dependent operation of seawater reverse osmosis. *Desalination*, 2010, 263, 76–88.

Gwenzi, W.; Musiyiwa, K.; Mangori, L. Sources, behaviour and health risks of antimicrobial resistance genes in wastewaters: A hotspot reservoir. *Journal of Environmental Chemical Engineering*, In press, corrected proof, Available online 19 February 2018.

Koroneos, C.; Dompros, A.; Roumbas, G. Renewable energy driven desalination systems modelling. *J. Cleaner Prod.,* 2007, 15, 449–464.

Krasner, S.W.; Mitch, W.A.; McCurry, D.L.; Hanigan, D.; Westerhoff, P. Formation, precursors, control, and occurrence of nitrosamines in drinking water: a review. *Water Res.*, 2013, 47, 4433–4450.

Krauss, M.; Longre´e, P.; Dorusch, F.; Ort, C. Hollender, J. Occurrence and removal of N nitrosamines in wastewater treatment plants. *Water Res.*, 2009, 43 (17), 4381–4391.

Krauss, M.; Longrée, P.; Van Houtte, E.; Cauwenberghs, J.; Hollender, J. Assessing the fate of nitrosamine precursors in wastewater treatment by physicochemical fractionation. *Environ. Sci. Technol*., 2010, 44, 7871–7877.

Lee, C.; Choi, W.; Kim, Y.G.; Yoon, J. UV photolytic mechanism of N-nitrosodimethylamine in water: Dual pathways to methylamine versus dimethylamine. *Environ. Sci. Technol.*, 2005, 39, 2101–2106.

Loutatidou, S.; Liosis, N.; Pohi, R.; Ouarda, T.; Arafat, H. A. Wind-powered desalination for strategic water storage: Techno-economic assessment of concept. *Desalination*, 2017, 408, 36–51.

Mane, P. P.; Park, P.-K.; Hyung, H.; Brown, J. C.; Kim, J.-H. Modelling boron rejection in pilot- and full-scale reverse osmosis desalination processes. *J. Membr. Sci.* 2009, 338, 119–127.

Magara, Y.; Tabata, A.; Kohki, M.; Kawasaki, M.; Hirose, M. Development of boron reduction system for sea water desalination. *Desalination*, 1998, 118, 25–33.

McCurry, D.L.; Ishida, K.; Oelker, G.; Mitch, W.A. Reverse Osmosis Shifts Chloramine Speciation Causing Re-Formation of NDMA during Potable Reuse of Wastewater. *Environ. Sci. Technol.*, 51 (15), 2017, 8589–8596.

Ministry of the Environment of Ontario, Technical support document for Ontario Drinking Water Standards, objectives and guidelines. as of January 2009, <http:// www.ene.gov.on.ca/envision/techdocs/4449e.htm>.

Najm, I; Trussell, R.R. NDMA formation in water and wastewater. *Journal (American Water Works Association)*, 2001, 93(2), 92–99.

Peñate, B.; Castellano, F.; Bello, A.; García-Rodríguez, L. Assessment of a stand-alone gradual capacity reverse osmosis desalination plant to adapt to wind power availability: A case study. *Energy*, 2011, 36, 4372–4384.

Plumlee, M.H.; Lo´pez-Mesas, M.; Heidlberger, A.; Ishida, K.P.; Reinhard, M. N-nitrosodimethylamine (NDMA) removal by reverse osmosis and UV treatment and analysis via LC–MS/MS. *Water Res.*, 2008, 42, 347–355.

Process System Enterprise Ltd. 2001. *gPROMS Introductory User Guide*. London: Process System Enterprise Ltd.

Redondo, J.; Busch, M.; De Witte, J. Boron removal from seawater using FILMTECTM high rejection SWRO membranes. *Desalination*, 2003, 156, 229–238.

Sarkar, P.; Goswami, D.; Prabhakar, S.; Tewari, P. K. Optimized design of a reverse osmosis system with a recycle. *Desalination*, 2008, 230, 128–139.

Schäfer, A.I.; Mitch, W.; Walewijk, S.; Munoz, A.; Teuten, E.; Reinhard, M. Chapter 7 micropollutants in water recycling: a case study of N-nitrosodimethylamine (NDMA) exposure from water versus food. *Sustainability Science and Engineering*, 2010, 2, 203–228.

Schwinge, J.; Neal, P. R.; Wiley, D. E.; Fletcher, D. F.; Fane, A. G. Spiral wound modules and spacers Review and analysis. *J. Membr. Sci.* 2004, 242, 129–153.

Sgroi, M.; Roccaro, P.; Oelker, G.L.; Snyder, S.A. N-nitrosodimethyl amine (NDMA) formation at an indirect potable reuse facility. *Water Res.* 2015, 70, 174–183.

Shi, M.; Wang, Z.; Zhao, S.; Wang, J.; Zhan, P.; Cao, X. A novel pathway for high performance RO membrane: Preparing active layer with decreased thickness and enhanced compactness by incorporating tannic acid into the support. *Journal of Membrane Science*, 2018, 555, 157–168.

Steinle-Darling, E.; Zedda, M.; Plumlee, M.H.; Ridgway, H.F.; Reinhard, M. Evaluating the impacts of membrane type, coating, fouling, chemical properties and water chemistry on reverse osmosis rejection of seven nitrosoalklyamines, including NDMA. *Water Res.*, 2007, 41, 3959–3967.

United States Environmental Protection Agency (US EPA), 2009. Office of Research and Development (ORD), National Center for Environmental Assessment. Integrated Risk Information System. U.S. Environmental Protection Agency, Washington, DC (http://www.epa.gov/iris/) (Accessed March 5, 2018).

Wei, Q. J.; McGovern, R. K.; Lienhard, J. H. Saving energy with an optimized two-stage reverse osmosis system. *Environmental Science: Water Research and Technology*, 2017, DOI: 10.1039/c7ew00069c.

World Health Organization (WHO), 2008. N-Nitrosodimethylamine (NDMA), in Guidelines for Drinking-Water Quality, 3rd Edition Including 1st and 2nd Addenda. (http://www.who.int/water_sanitation_health/dwq/chemicals/ndmasummary_2ndadd.pdf) (Accessed March 5, 2018).

Zhou, W.; Song, L. Experimental study of water and salt fluxes through reverse osmosis membranes. *Environ. Sci. Technol.* 2005, 39, 3382–3387.

Appendix A

Table A.1. The mathematical modelling of a single spiral wound RO system

Model Equations	Specifications	Eq. no.
$J_w = A_{w(T)}\left[\left(\frac{(P_{f(in)}+P_{f(out)})}{2} - P_p\right) - (\Delta\pi_{Total})\right]$	The permeate flux	1
$\Delta\pi_{Total} = (\pi_m - \pi_p)$	The total osmotic pressure	2
$\pi_w = 1.19\,(T + 273.15)\left(\frac{C_w}{Mwt}\right)$	The osmotic pressure of NDMA at the membrane wall concentration	3
$\pi_p = 1.19\,(T + 273.15)\left(\frac{C_p}{Mwt}\right)$	The osmotic pressure at permeate channel regarding the permeate concentration	4
$J_s = B_{s(T)}\,(C_w - C_p)$	The solute flux	5
$\frac{(C_w - C_p)}{(C_b - C_p)} = exp\left(\frac{J_w}{k}\right)$	The wall solute concentration	6
$k = 0.753\left(\frac{K}{2-K}\right)^{0.5}\left(\frac{D_b}{t_f}\right)\left(\frac{\mu_b\,\rho_b}{D_b}\right)^{0.1666}\left(\frac{2\,t_f^2\,U_b}{D_b\,\Delta L}\right)^{0.5}$	The mass transfer coefficient (Mane *et al.*, 2009)	7
$D_b = 6.725E-6\,exp\left\{0.1546E-3\,C_b) - \frac{2513}{(T+273.15)}\right\}$	The diffusivity parameter at the feed channel (Koroneos, 2007)	8
$\mu_b = 2.141E-5x10^{\left(\frac{247.8}{(T+273.15)-140)}\right)}$	The dynamic viscosity at the feed channel (Fujioka *et al.*, 2014)	9
$\rho_b = 498.4\,m_f + \sqrt{[248400\,m_f^2 + 752.4\,m_f\,C_b]}$	The feed density ((Koroneos, 2007)	10
$m_f = 1.0069 - 2.757E-4\,T$	Parameter in Eq. (10)	11
$Re = \frac{\rho_b\,d_h\,U_b}{\mu_b}$	The Reynolds number at the feed channel	12
$U_b = \frac{Q_b}{W\,t_f\,\epsilon}$	The bulk feed velocity	13
$Q_b = \frac{Q_f + Q_r}{2}$	The bulk feed flow rate	14
$C_b = \frac{C_f + C_r}{2}$	The bulk concentration	15
$C_p = \frac{C_f\;B_{s(T)}}{B_{s(T)} + \frac{J_w}{\exp(\frac{J_w}{k})}}$	The permeate solute concentration (Al-Obaidi *et al.*, 2017a)	16
$Q_f = Q_r + Q_p$	The retentate flow rate	17
$Q_f\,C_f = Q_r\,C_r + Q_p\,C_p$	The retentate concentration	18
$Q_p = J_w\,A$	The total permeated flow rate	19
$P_{f(out)} = P_{f(in)} - \Delta P_{drop}$	The retentate pressure	20
$\Delta P_{drop} = \left(\frac{\rho_b\;U_b^2\,L\,C_{td}}{2\,d_h}\right)\,x9.8692e-6$	The pressure drop per each membrane (Da Costa *et al.*, 1994)	21

$C_{td} = \frac{A'}{Re^n}$	The total drag coefficient	22

Table A.1. The mathematical modelling of a single spiral wound RO system (Continued)

Model Equations	Specifications	Eq. no.
$Re = \frac{U_b\, d_h\, \rho_b}{\mu_b}$	The Reynolds number	
$Rec = \frac{Q_p}{Q_f}\, x100$	The total permeate recovery	23
$Rej = \frac{C_f - C_p}{C_f} x100$	The solute rejection	24
$E1 = \frac{\left(P_{f(in)}\, x101325)\, Q_f\right)}{\frac{Qp\ \varepsilon pump}{36E5}}$	The total plant energy consumption with high-pressure pump	25
$E2 = \frac{\left(P_{f(in)}\, x101325)\, Q_f\right)}{\frac{Qp\ \varepsilon pump}{36E5}} - \frac{(P_{f(out)}\, x101325)\ Q_r\, \varepsilon_{ERD}}{Qp}$	The total plant energy consumption with high-pressure pump and ERD	26
$\varepsilon_{ERD} = \frac{P_{f(out)(ERD)}}{P_{f(in)(ERD)}}$	The efficiency of energy recovery device	27
$A_{w(T+273.15)} = A_{w(T_{ref}+273.15)} \frac{\mu_{b(T_{ref}+273.15)}}{\mu_{b(T+273.15)}}$	The impact of temperature on water permeability constant (Sarkar *et al.*, 2008)	28
$B_{s(T+273.15)} = B_{s(T_{ref}+273.15)} \frac{T+273.15}{T_{ref}+273.15} \frac{\mu_{b(T_{ref}+273.15)}}{\mu_{b(T+273.15)}}$	The impact of temperature on solute permeability constant (Sarkar *et al.*, 2008)	29

Table A.2. The parameter estimation results

$A_{w(T)}$ (m/s atm)	$B_{s(T)}$ (m/s)	A' (dimensionless)	n (dimensionless)
1.1290E-6	4.0919E-6	1.47	0.24

Table A.3. The model validation results

$P_{f(in)}$ (atm)	J_w (m/s)		Error %	Q_r (m³/s)		Error %	Rej (-)		Error %
	Exp.	Model		Exp.	Model		Exp.	Model	
4	2.78E-6	2.733E-6	1.67	2.36E-3	2.365E-3	-0.22	0.388	0.3903	-0.60
6.51	5.56E-6	5.583E-6	-0.41	2.30E-3	2.297E-3	0.100	0.561	0.5555	0.96

$C_{f(NDMA)} = 250$ ng/l, $Q_f = 2.43E-3$ m³/s, and $T = 20$ °C

Table A.4. Simulation results of twelve scenarios of retentate reprocessing RO networks

Scenario	Rej_{plant} (-)	Rec_{plant} (-)	$E1$ (kWh/m³)
D	39.709	76.548	0.597
E	39.148	77.295	0.591
F	39.437	76.967	0.594
G	38.852	78.277	0.584
H	38.743	78.698	0.581

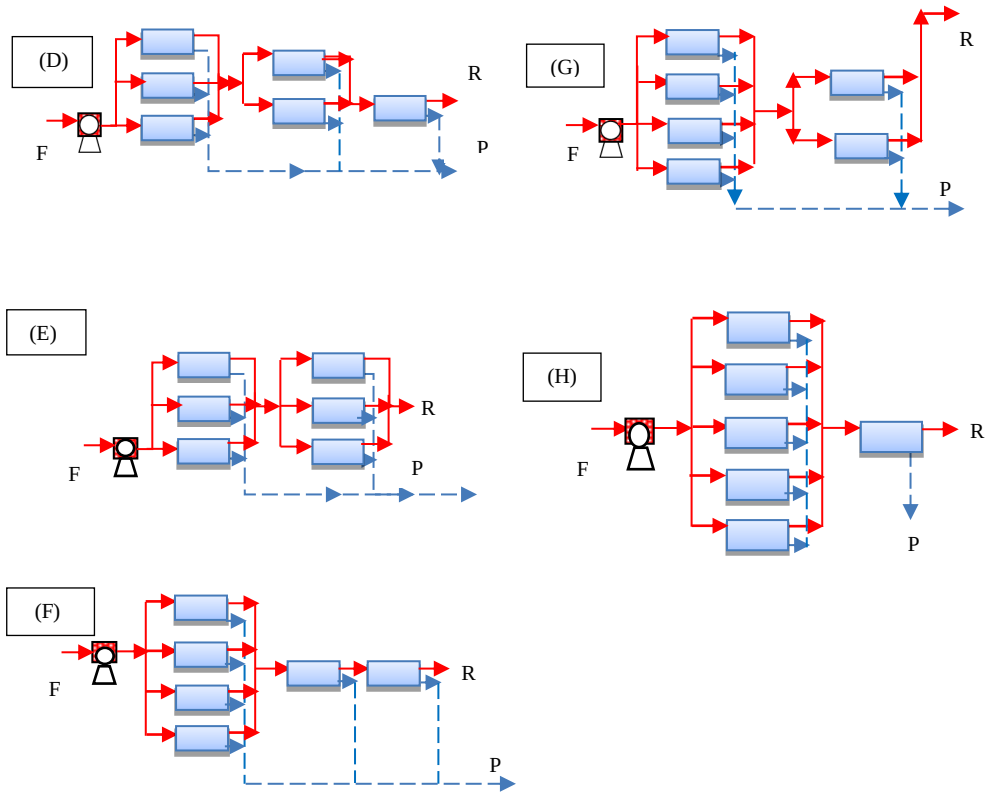

Fig. A.1. The tested configurations of retentate reprocessing RO networks of six pressure vessels (F: Feed, P: permeate, R: Retentate)